

Jacky S. H. Lee · Dongqing Li

Electroosmotic flow at a liquid–air interface

Received: 12 December 2005 / Accepted: 20 January 2006 / Published online: 16 February 2006
© Springer-Verlag 2006

Abstract This paper presents the first experimental evidence on electroosmotic flow at a liquid–air interface. A PDMS microchannel with an opening to air was created to allow for the formation of a liquid–air interface. Polystyrene particles were used to visualize the liquid motion and the experiments found that the particle velocity at the liquid–air interface was significantly slower than the particle velocity in the bulk. This result agrees with a mathematical model that considers the effects of electrical surface charges at the liquid–air interface in electroosmotic flow.

Keywords Free surface electroosmotic flow · Electroosmotic flow · Two-phase flow · Electrophoresis

1 Introduction

Electroosmotic flow in microchannel systems has been studied extensively over the past decade. Electroosmotic flow occurs because of the presence of the electrical double layer (EDL), which can be well described by the widely accepted Gouy–Chapman–Stern model. Electroosmotic flow allows for precise liquid manipulation in a complex microchannel network. It is also generally known that electroosmotic flow has a plug-like velocity profile.

Multi-phase microfluidic systems have attracted attentions from researchers. Many of the systems investigated involved oil droplet transport in microchannels (Marsh et al. 2004; Kevin et al. 2000). Recently, studies of using electroosmotic flow to pump

indirectly non-polar liquid were also conducted (Brask et al. 2003; Gao et al. 2005a, b). However, the theory for electroosmotic flow in microchannels is insufficient in fully describing the characteristic of electroosmotic flow involving a liquid–fluid interface. The current Gouy–Chapman–Stern model assumes the liquid is in contact with a solid and the liquid and ions at the solid–liquid interface are assumed to be immobile. In a liquid–fluid two-phase system, the liquid is in contact with another fluid phase. The interface is no longer immobile, and the ions at the interface are mobile. The movement of ions at the liquid–fluid interface must be taken into consideration in the EDL model and the transport phenomena model. To date, there has been very little discussion on the physics of electroosmotic flow near an interface of two immiscible fluids. Brask et al. (2003) and Gao et al. (2005a, b) have theoretically investigated to two-phase electroosmotic flow; however, neither physical explanation nor justification was provided.

Recently, the authors of this paper have analyzed the different theoretical models proposed for two-phase electroosmotic flow and evaluated them against experimental evidence (Lee et al. 2005). The results show that the effect of surface charges must be considered along with the Gouy–Chapman–Stern model to produce results closed to that in experiments. This theoretical model predicts that if the liquid–fluid interface zeta potential is of the same sign as the microchannel walls' zeta potential, then the liquid electroosmotic velocity at the liquid–fluid interface would be slower than the velocity in the bulk flow. In the case of a water–air interface, where the zeta potential of water–air interface is approximately -65 mV (Graciaa et al. 1995) and the zeta potential of glass is approximately -86 mV (Erickson et al. 2000), the interface fluid electroosmotic velocity is significantly slower than the bulk fluid electroosmotic velocity. The author's previous work relies on comparing the velocity profiles in the bulk flow region, thus, did not provide direct evidence of the velocity at the liquid–fluid interface. The purpose of this work is to provide the first experimental evidence on the liquid

J. S. H. Lee
Department of Mechanical and Industrial Engineering,
University of Toronto, 5 King's College Road, Toronto,
Ont., M5S 3G8, Canada

D. Li (✉)
Department of Mechanical Engineering, Vanderbilt University,
VU Station B 351592, Nashville, TN 37235-1592, USA
E-mail: dongqing.li@vanderbilt.edu

electroosmotic velocity at the interface between two immiscible fluids; more specifically, the electroosmotic velocity at a liquid–air interface.

2 Experimental device

The experiments involved a specially designed PDMS microchannel with an opening to allow the liquid to interface with air. Figure 1 illustrates the PDMS structure used in the experiments. The rectangular microchannel structure in PDMS was molded from a positive SU-8 master created by standard soft-photolithography process (Xia et al. 1998). Two different sizes of the microchannel (i.e., microchannel's cross-sectional dimensions) were used in this study, 100 μm by 100 μm and 50 μm by 50 μm . The bottom pieces of the PDMS channel were created in the following way. First we use plasma to treat a piece of flat PDMS to make the surface hydrophilic. Then, this piece was cut into two and before they were bonded to another piece of plasma treated PDMS with the microchannel structure. This procedure helped prevent liquid leaking through the edges of the bottom PDMS. The separation of the bottom pieces was 5 mm. Finally, the whole PDMS structure was placed on a microscope slide. When liquid was filled through the microchannel, a liquid–air interface would form in the air gap of the microchannel due to surface tension. The curvature of this interface was calculated to be in the order of centimeters from the Laplace–Young equation. Therefore, it is assumed flat in microscale.

The 0.5 μm fluorescence polystyrene particles (Bang Laboratories Inc., IN, USA) were used to visualize the liquid flow. Prior to use, the particles were diluted at 0.5% v/v ratio in the working solutions. The particle

motions were captured with a Leica DMLM fluorescent microscope with a 32 \times air objective lens, a Retiga 12-bit cooled CCD camera and OpenLab 3.1.5 image acquisition software. The focus plane of the objective lens has a thickness of approximately 10 μm . Two sets of images were captured: first set of images focused at the midpoint of the microchannel (e.g., 50 μm away from the liquid–air interface), and the second set of images focused at the liquid–air interface. Consecutive images were taken at a frame rate of 0.2 s. These images were digitalized and the distances between particles for consecutive images were measured using the OpenLab software to calculate their speed.

The zeta potential of PDMS with working solutions was measured using the current monitoring method (Sze et al. 2003). The electrophoretic mobility of particles was calculated by comparing the observed particle velocities and the measured fluid velocities from the current monitoring method. To this date, there has been no study on the particle electrophoretic mobility at an immiscible liquid interface; therefore, the electrophoretic mobility of the particles in the bulk region and that in the interface region are assumed to be the same. The effects of this assumption are discussed in the following section. In order to compare experimental results with theoretical predictions, the zeta potentials of PDMS and water–air interface must be known. The zeta potential for deionized water and 1 mM NaCl in oxidized PDMS channels was measured to be -98 and -85 mV, respectively. The zeta potential for deionized water and 1 mM NaCl at a liquid–air interface were found to be ~ 65 mV (Graciaa et al. 1995) and -40 mV (Yang et al. 2001). The electrophoretic mobility of the particles in deionized water and 1 mM NaCl were calculated to be $-1.53 \times 10^{-8} \pm 0.2 \times 10^{-8}$ and $-2.3 \times 10^{-8} \pm 0.3 \times 10^{-8}$ m²/V/s, respectively.

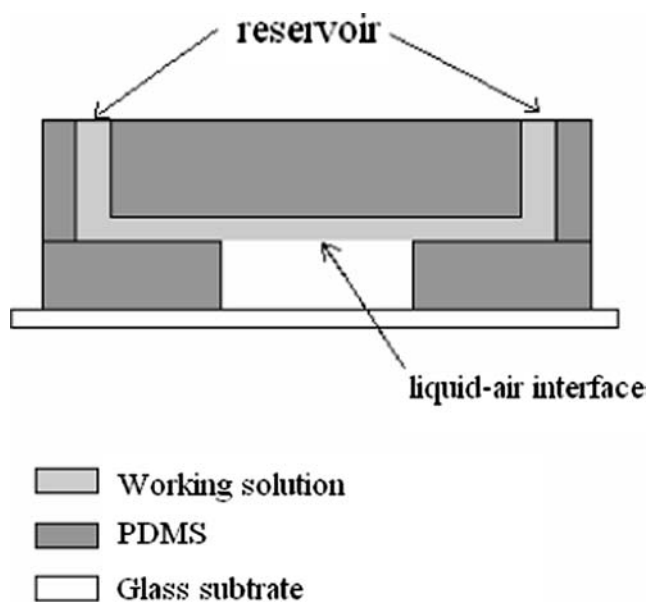
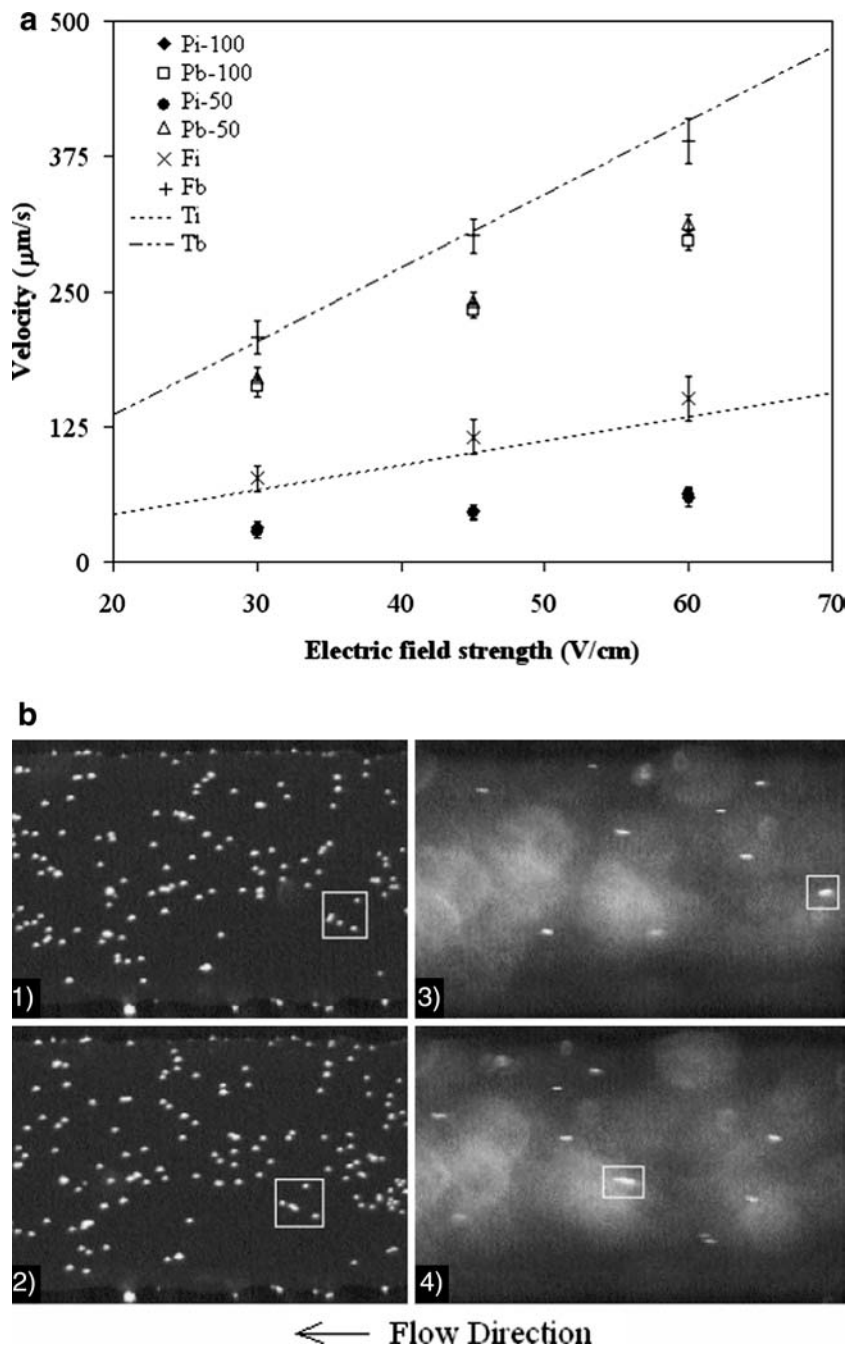


Fig. 1 Schematics of the PDMS microchannel with an opening to allow for the formation of a liquid–air interface

3 Observation and discussion

This study investigated two working fluids: Pure deionized water and 1 mM NaCl solution at pH 7. Particles were diluted in the working solutions and were injected to the reservoirs of the microchannel. The particles near the liquid–air interface region were attracted and trapped by the interface. This phenomenon of particles attachment at a liquid–air interface was commonly observed in the literature (Yang et al. 1999; Fan et al. 2004; Drzymala 1999; Ralston et al. 1999). When an external electric field was applied, both the particles in the bulk liquid and at the liquid interface would move. Figure 2a shows the effects of applied electric field and channel size on the particle velocities for the deionized water system. The fluid velocity was calculated by $u_{\text{fluid}} = u_{\text{observed}} + \mu_{\text{ep}}E$, where u_{fluid} , u_{observed} , and $\mu_{\text{ep}}E$ are the calculated fluid velocity, the observed particle velocity, and the electrophoretic velocity of particles. The calculated velocities were compared against the fluid velocities predicted by the

Fig. 2 a Particle and calculated fluid velocity as a function of electric field strength in deionized water. Pi-100 and Pb-100 are the particle velocities at the water–air interface and in the bulk liquid for a 100 μm by 100 μm microchannel, respectively. Pi-50 and Pb-50 are the particle velocities at the water–air interface and in the bulk liquid for a 50 μm by 50 μm microchannel, respectively. Fi and Fb are the calculated fluid velocities ($u_{\text{fluid}} = u_{\text{observed}} + \mu_{\text{ep}} E$) at the water–air interface and in the bulk liquid for a 100 μm by 100 μm microchannel, respectively. Ti and Tb are the predicted fluid velocities at the water–air interface and in the bulk liquid by the theoretical model (Lee et al. 2005). **b** Image sequences of electroosmotic flow at a water–air interface and in the bulk liquid. Images 1 and 2 are the sequence images for electroosmotic flow at a water–air interface. Images 3 and 4 are the sequence images for electroosmotic flow in the bulk liquid. The time lapse between the respective successive images is 0.4 s. The electric field strength is 30 V/cm

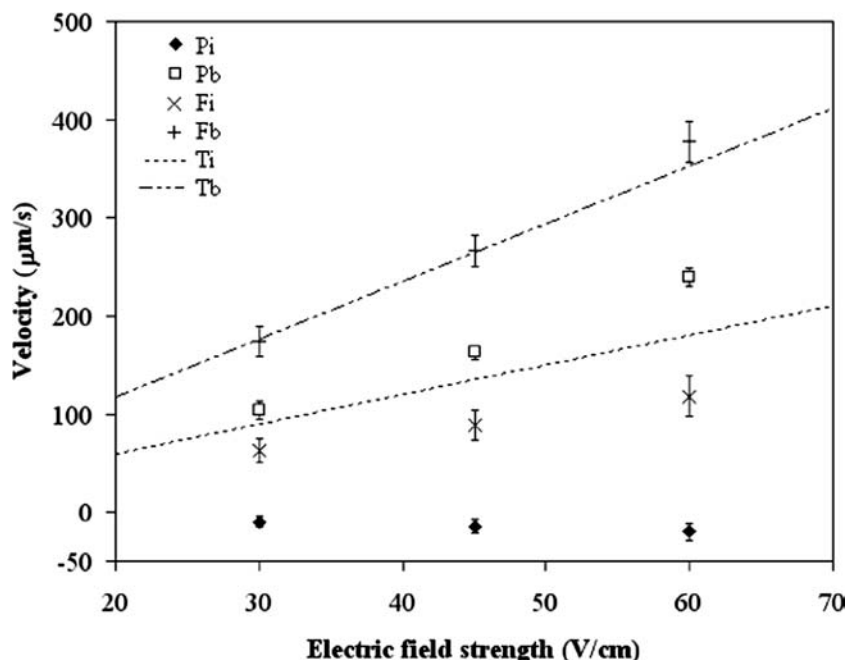


model presented in Lee et al. (2005) and Gao et al. (2005a, b). The particle velocity in the bulk and the liquid interface regions is found to increase linearly with applied electric field. In addition, the channel size (50–100 μm in width) is found to have no effects on the particle velocity. Under the assumption of equal particle electrophoretic mobility in the bulk and liquid interface regions as mentioned, the calculated fluid velocities at the interface match the predicted velocity with good accuracy. Furthermore, in Fig. 2b, it can be clearly seen that the particles at the water–air interface traveled at a much slower speed. This is the first direct evidence that compares the electroosmotic flow at a

liquid interface and the bulk electroosmotic flow. The physical explanation for the reduction in fluid speed at the interface is that the surface charges at the liquid interface will impose a surface shear stress counter acting the flow under an applied electric field. This stress, similar to the viscous stress in liquids near a solid surface, slows down the liquid. More details on the physical description on the model can be found in Lee et al. (2005).

Figure 3 shows the particle velocities and calculated fluid velocities for 1 mM NaCl solution. For this case, a significant speed reduction at the liquid interface was also observed. From the theoretical model (Lee et al.

Fig. 3 Particle velocity and the calculated fluid velocity for 1 mM NaCl solution in a 100 μm by 100 μm microchannel. Pi-100 and Pb-100 are the particle velocities at the liquid–air interface and in the bulk fluid, respectively. Fi and Fb are the calculated fluid velocities ($u_{\text{fluid}} = u_{\text{observed}} + \mu_{\text{ep}}E$) at the liquid–air interface and in the bulk liquid, respectively. Ti and Tb are the predicted fluid velocity at the liquid–air interface and in the bulk liquid by the theoretical model (Lee et al. 2005)



2005), the reduction in fluid speed occurs only inside the EDL. Since the thickness of the EDL is in the order of 10 nm for 1 mM NaCl solution, this experimental result indicates that the particles are indeed attached to the liquid interface. The results show that the calculated electroosmotic velocities at the interface are lower than the predicted bulk electroosmotic velocities. Furthermore, the particles' electrophoretic speed at the liquid interface increases with the applied electric field but in the opposite (negative velocity) direction to the liquid electroosmotic flow. As a result, the observed particle velocity is negative as shown in Fig. 3. Figure 3 also shows the comparison between the calculated and predicted liquid velocity. Note again that the calculated liquid velocity is determined by $u_{\text{fluid}} = u_{\text{observed}} + \mu_{\text{ep}}E$. The bulk velocities compare very well; however, there is a larger discrepancy in the liquid interface velocities than that in the case shown in Fig. 2a. The possible reasons are discussed below.

In this study, the electrophoretic mobility of particles at the liquid interface and in the bulk flow is assumed to be equal. However in reality, this may not be the case. The electrophoretic mobility is dependent on dielectric constant, the zeta potential of particle and viscosity of fluid. Since the zeta potential is dependent on the ionic concentration of both co-ions and counter-ions, the particles at the liquid–air interface may have non-uniform zeta potentials because the ions distribution at a liquid–air interface is non-uniform (Garrett 2004). Second, the electrical properties (such as dielectric constant) and fluid properties (such as viscosity) at the interface may be different from the bulk (Paluch 2000). Third, there are more complicated phenomena such as EDL interaction between particles and a liquid interface, which would further complicate the electrophoresis at a

liquid–air interface. All these coupled effects would affect the electrophoretic mobility of a particle at a liquid–fluid interface. Clearly, a more in-depth study of particle motion at a liquid–fluid interface is needed. Nevertheless, this work provides the first experimental evidence on velocity measured at a liquid–air interface under an applied electric field and shows that velocity at a liquid–air interface is slower than the bulk flow.

4 Conclusion

Experiments were conducted to examine the electroosmotic flow at the liquid–air interface. Results show that there was a significant reduction in the particle electrokinetic velocity and the electroosmotic velocity of the fluid at the liquid–air interface, in comparison with that in the bulk liquid. This result agrees with a theoretical model that includes the effects of electrical surface charges in the electroosmotic flow model.

Acknowledgments The authors are thankful for the financial support of the National Sciences and Engineering Research Council through a research grant to D. Li and scholarships to J. Lee.

References

- Brask A, Goranovic G, Bruus H (2003) Electroosmotic pumping of nonconducting liquids by viscous drag from a secondary conducting liquid. *Tech Proc Nanotech* 1:190–193
- Drzymala J (1999) Entrainment of particles with density between 1.01 and 1.10 g/cm^3 in a monobubble hallimond flotation tube. *Miner Eng* 12:329–331
- Erickson D, Li D, Werner C (2000) An improved method of determining the zeta-potential and surface conductance. *J Colloid Interface Sci* 232:186–197

- Fan X, Zhang Z, Li G, Rowson NA (2004) Attachment of solid particles to air bubbles in surfactant-free aqueous solutions. *Chem Eng Sci* 59:2639–2645
- Gao Y, Wong TN, Yang C, Ooi KT (2005a) Transient two-liquid electroosmotic flow with electric charges at the interface. *Colloids Surf A* 266:117–128
- Gao Y, Wong TN, Yang C, Ooi KT (2005b) Two-fluid electroosmotic flow in microchannels. *J Colloid Interface Sci* 284:306–314
- Garrett BC (2004) Ions at the air/water interface. *Science* 303:1146–1147
- Graciaa A, Morel G, Saulner P, Lachaise J, Schechter RS (1995) The zeta-potential of gas bubbles. *J Colloid Interface Sci* 172:131–136
- Kevin D, Altria (2000) Background theory and applications of microemulsion electrokinetic chromatography. *J Chromatogr A* 892:171–186
- Lee JSH, Barbulovic-Nad I, Wu Z, Xuan X, Li D (2005) Electrokinetic flow in a free surface-guided microchannel. *J Appl Phys* (in press)
- Marsh A, Clark B, Broderick M, Power J, Donegan S, Altria K (2004) Recent advances in microemulsion electrokinetic chromatography. *Electrophoresis* 25:3970–3980
- Paluch M (2000) Electrical properties of free surface of water and aqueous solutions. *Adv Colloid Interface Sci* 84:27–45
- Ralston J, Dukhin SS (1999) The interaction between particles and bubbles. *Colloids Surf A* 151:3–14
- Sze A, Erickson D, Ren L, Li D (2003) Zeta-potential measurement using the Smoluchowski equation and the slope of the current–time relationship in electroosmotic flow. *J Colloid Interface Sci* 261:402–410
- Xia Y, Whitesides GM (1998) Soft lithography. *Annu Rev Mater Sci* 28:153–184
- Yang C, Dabros T, Li D, Czarnecki J, Masliyah JH (1999) Analysis of fine bubble attachment onto a solid surface within the framework of classical DLVO theory. *J Colloid Interface Sci* 219:69–80
- Yang C, Dabros T, Li D, Czarnecki J, Masliyah JH (2001) Measurement of the zeta potential of gas bubbles in aqueous solutions by microelectrophoresis method. *J Colloid Interface Sci* 243:128–135